

1

2

3 Main Manuscript for

4 Reconstructing Middle and Upper Palaeolithic human mobility in 5 Portuguese Estremadura through laser ablation strontium isotope 6 analysis

7 Bethan Linscott^{1,2*}, Alistair W.G. Pike^{2*}, Diego E. Angelucci^{3,4}, Matthew J. Cooper⁵, J Andy
8 Milton⁵, Henrique Matias⁴, João Zilhão^{4,6,7}

9 ¹Oxford Radiocarbon Accelerator Unit, University of Oxford, UK.

10 ²Department of Archaeology, University of Southampton, UK.

11 ³Dipartimento di Lettere e Filosofia, Università degli Studi di Trento, Italy.

12 ⁴UNIARQ, Centro de Arqueologia da Universidade de Lisboa, Portugal.

13 ⁵School of Ocean and Earth Science, NOCS, University of Southampton, UK.

14 ⁶ICREA, Barcelona, Spain.

15 ⁷Department of History and Archaeology, University of Barcelona, Spain

16 *Corresponding authors

17 *Paste corresponding author name(s) here.

18 **Email:**

19 bethan.linscott@arch.ox.ac.uk

20 a.w.pike@soton.ac.uk

21 PNAS strongly encourages authors to supply an [ORCID identifier](#) for each author. Do not include
22 ORCIDs in the manuscript file; individual authors must link their ORCID account to their PNAS
23 account at www.pnascentral.org. For proper authentication, authors must provide their ORCID at
24 submission and are not permitted to add ORCIDs on proofs.

25 **Author Contributions:** AWGP, BL, JZ, DEA, and HM designed the research and collected the
26 samples. BL, AWGP, JZ, MJC and AM undertook the isotopic analyses. All authors interpreted the
27 results and prepared the manuscript.

28 **Competing Interest Statement:** None.

29 **Classification:** BIOLOGICAL SCIENCES - Anthropology

30 **Keywords:** MIDDLE PALAEOLITHIC, UPPER PALAEOLITHIC, PORTUGAL, MOBILITY, STRONTIUM
31 ISOTOPES.

32 **This PDF file includes:**

33 Main Text
34 Figures 1 to 4
35

36 **Abstract**

37 Understanding mobility and landscape use is important in reconstructing subsistence behaviour,
38 range, and group size, and it may contribute to our understanding of phenomena such as the
39 dynamics of biological and cultural interactions between distinct populations of Upper
40 Pleistocene humans. However, studies using traditional strontium isotope analysis are generally
41 limited to identifying locations of childhood residence or non-local individuals, and lack the
42 sampling resolution to detect movement over short timescales. Here, using an optimised
43 methodology, we present highly spatially resolved $^{87}\text{Sr}/^{86}\text{Sr}$ measurements made by laser
44 ablation multi-collector inductively coupled plasma mass spectrometry (LA-MC-ICP-MS) along
45 the growth axis of the enamel of two Marine Isotope Stage (MIS) 5b, Middle Palaeolithic
46 Neanderthal teeth (Gruta da Oliveira), a Tardiglacial, Late Magdalenian human tooth (Galeria da
47 Cisterna) and associated contemporaneous fauna from the Almonda karst system, Torres Novas,
48 Portugal. Strontium isotope mapping of the region shows extreme variation in $^{87}\text{Sr}/^{86}\text{Sr}$, with
49 values ranging from 0.7080 to 0.7160 over a distance of c. 50 km, allowing short distance (and
50 arguably short-duration) movement to be detected. We find that the early Middle Palaeolithic
51 individuals roamed across a subsistence territory of approximately 600 km², while the Late
52 Magdalenian individual parsimoniously fits a pattern of limited, probably seasonal movement
53 along the right bank of the 20 km-long Almonda River valley, between mouth and spring,
54 exploiting a smaller territory of approximately 300 km². We argue that the differences in
55 territory size are due to an increase in population density during the Late Upper Palaeolithic.

56 **Significance Statement**

57 Laser ablation MC-ICP-MS allows in-situ strontium isotope data to be obtained for incrementally
58 formed biapatites such as enamel with extremely high spatial resolution. Here, we provide the
59 first large scale application of the method comparing the mobility and subsistence behaviour of
60 Middle and Upper Palaeolithic humans in the same landscape. These remains and the fauna
61 analysed alongside come from the Almonda karst system (Portuguese Estremadura). Data
62 suggest that regional Middle Palaeolithic individuals roamed across a subsistence territory of
63 approximately 600 km², whilst Upper Palaeolithic individuals moved seasonally and exploited a
64 smaller territory of approximately 300 km².

65

66 **Main Text**

67

68 **Introduction**

69

70 Understanding the mobility patterns of Middle and Upper Palaeolithic human populations can
71 aid in the reconstruction of their subsistence behaviour, cognitive ability, geographical range,

72 and group size. In particular, diachronic comparisons of landscape use and subsistence
73 strategies of anatomically modern humans (AMH) and Neanderthals may provide insights into
74 the factors that led to the assimilation of the latter in Europe approximately 45,000 – 40,000
75 years ago (1). The Iberian Peninsula occupies a central position in debates concerning the
76 interaction between these two human groups around the Middle-Upper Palaeolithic transition
77 (2-6), but direct isotopic studies of Middle and Upper Palaeolithic human and animal mobility
78 from this region have so far been limited.

79 Strontium isotope analysis of bulk enamel is a routine methodology for exploring past mobility
80 (7), but until the application of LA-MC-ICP-MS analysis (8-10), the sample size required
81 precluded its application to intra tooth Sr isotope analysis on human material. Now, the spatial
82 resolution of optimised laser ablation MC-ICP-MS analysis allows >1000 individual $^{87}\text{Sr}/^{86}\text{Sr}$
83 measurements along a typical human enamel sample (11). This method, when combined with
84 sequential oxygen isotope analysis, can provide seasonal mobility data for humans and fauna in
85 areas where geological variation is significant across short distances. By combining indirect
86 evidence for settlement patterns and resource exploitation (such as faunal assemblages and
87 lithics) with isotopic data, a more detailed picture of the subsistence behaviours of human
88 groups can be developed.

89 The Pleistocene cave deposits of Portuguese Estremadura's Central Limestone Massif offer an
90 invaluable opportunity to carry out such a study *ceteris paribus* because of the region's highly
91 variable, patchwork geology. Two localities therein, the Almonda karst system (Torres Novas)
92 and the Gruta do Caldeirão (Tomar), provide one of the richest collections of Middle and Late
93 Pleistocene human and animal remains in western Iberia, characterised by human remains
94 dating to the Lower, Middle and Upper Palaeolithic (6, 12-15). Here, we present sequential,
95 high-resolution strontium isotope data for the tooth enamel of three individuals from the
96 Almonda karst system (two Neanderthals from Gruta da Oliveira and a Magdalenian human
97 from Galeria da Cisterna) obtained through LA-MC-ICP-MS analysis, along with sequential
98 strontium and oxygen isotope data for contemporaneous fauna from the Almonda sites (Table
99 S1).

100

101 **Methodological background**

102 The $^{87}\text{Sr}/^{86}\text{Sr}$ ratio of bedrock is a function of the initial ^{87}Rb content and time elapsed since its
103 formation (7), and as such, rocks of different geological ages will exhibit distinct $^{87}\text{Sr}/^{86}\text{Sr}$ values.
104 The process of weathering introduces strontium ions from the underlying geology into the
105 biosphere — soils reflect the $^{87}\text{Sr}/^{86}\text{Sr}$ ratios of the bedrock from which they are derived, and
106 groundwater echoes the strontium isotope signal of deposits through which it passes (16). Local
107 soil and water $^{87}\text{Sr}/^{86}\text{Sr}$ ratios are subsequently adopted by the tissues of plants growing within a
108 given catchment, and these values are passed along the food chain from producer to consumer
109 with minimal fractionation (17-18). Strontium readily substitutes for calcium in calcium-bearing
110 minerals due to both cations sharing the same valency (19). The calcium component of the
111 primary mineral phase present in animal bones and teeth, hydroxyapatite ($\text{Ca}_{10}(\text{PO}_4)_6(\text{OH})_2$), is
112 therefore commonly replaced by strontium during biomineralization (20). Strontium and
113 calcium are metabolised by animals in the same way, and as such, teeth and bones will reflect
114 the $^{87}\text{Sr}/^{86}\text{Sr}$ ratios of food and water consumed during the formation or remodeling of these
115 respective tissues (19, 21). As such, the $^{87}\text{Sr}/^{86}\text{Sr}$ ratios observed in incrementally-formed,

116 biomineralised tissues of a given organism should primarily echo the isotopic signal of the
117 underlying geology of the area in which said tissue was formed or remodeled, allowing mobility
118 across geologies of varying age to be detected through sequential analysis. For archaeological
119 studies, the assumption is that baseline strontium isotopic values sampled today (e.g. from
120 plants or sediments) reflect those of the past. Problems with this assumption, e.g. from changes
121 in erosion patterns, can cause uncertainties in the interpretation of mobility.

122 The strontium isotopes in teeth will reflect the strontium-weighted mean of the dietary
123 components, which need to be considered. While it is acknowledged that Neanderthals
124 occupied a high trophic level, at least in the steppe-tundra regions of north-western Europe (e.g.
125 22), the bio-purification of strontium with trophic level means that meat is significantly
126 depleted in strontium relative to plants. A study of modern dietary strontium (23) shows that
127 nuts contain c. 74x the strontium of red meat; pulses (c.20x); vegetables (c.16x); cereals and
128 fruit (c. 9.5x). Furthermore, rabbit and poultry contain less strontium than red meat. It is likely,
129 therefore, that our strontium isotope measurements in human enamel are strongly weighted to
130 the locations of plant gathering rather than the migratory ranges of the animal species
131 consumed, although we acknowledge that some uncertainty remains.

132 The oxygen isotope composition of precipitation differs as a result of variables including
133 altitude, latitude, rainout relating to the distance from the coast and air temperature (24). The
134 latter of these parameters, air temperature, varies with the seasons in mid and high latitudes.
135 The highest $\delta^{18}\text{O}$ values correlate with the warmest seasonal temperatures, and the lowest $\delta^{18}\text{O}$
136 values are associated with the coldest (25). Animal body water reflects the oxygen isotope
137 composition of the meteoric water ingested directly or indirectly by the individual, and as such,
138 those $\delta^{18}\text{O}$ values are incorporated by mammalian tissues as they form (ibid). Seasonal
139 temperature variations in rainfall $\delta^{18}\text{O}$ are therefore recorded as sinusoidal profiles in
140 incrementally formed tissues that develop over the course of a year or longer. Conversely, if an
141 individual engages in migratory behaviour, the measured $\delta^{18}\text{O}$ profile may appear flat or
142 dampened since the act of avoiding climatic extremes ensures a degree of stability in
143 experienced environmental conditions (26).

144 Since mammalian tooth enamel forms incrementally during childhood and is not subsequently
145 remodeled (20), it provides an invaluable time-resolved archive of biogeochemical information
146 that can be accessed if sufficiently high sampling resolution can be achieved. The rate and
147 geometry of the complex process of enamel mineralisation in diphyodont mammals has,
148 however, been a topic of debate with regard to its implications for the recovery of time-resolved
149 isotope data (27). Recent work on modern caprine tooth enamel combining LA-MC-ICP-MS
150 analysis and GPS tracking has nevertheless demonstrated that sequential $^{87}\text{Sr}/^{86}\text{Sr}$ can be used to
151 track mobility with a monthly resolution, at least in sheep and ibex (28). Whilst the
152 mineralization rate of human enamel is less well understood, spatially resolved $\delta^{18}\text{O}$ analyses of
153 Neanderthal teeth from Payre, France (29) have demonstrated that seasonal variations in
154 oxygen isotope values in single teeth are consistent with well documented modern human
155 crown formation times (30). A recent study of $^{87}\text{Sr}/^{86}\text{Sr}$ profiles in modern and archaeological
156 human tooth enamel has further demonstrated that chronologically sequenced ablation data
157 are not the result of end-member mixing, and can be considered reflective of transitions
158 between bioavailable strontium sources (31). Here, we present mobility of fauna at the seasonal

159 scale by anchoring $^{87}\text{Sr}/^{86}\text{Sr}$ data to $\delta^{18}\text{O}$ where possible. Additional information on our approach
160 and the methods used can be found in the *SI Appendix* (Text S1-S2).

161 **Site Background**

162 The Almonda karst system (Fig 1 and Figs. S1-S2) is located approximately 100 km to the north-
163 east of Lisbon, at the southern edge of the Mesozoic Central Limestone Massif of Portuguese
164 Estremadura. It consists of around 12 km of mapped subterranean galleries in association with
165 the spring of the Almonda River, which are accessed by multiple entrances — fossil outlets —
166 located at successive elevations up a limestone escarpment (Figs. S3-S4). The latter is part of the
167 ~40 km-long, NE-SW-oriented tectonic fault separating the massif's mountains and plateaus
168 from the Cenozoic alluvial plain of the Tagus River.

169 The Gruta da Oliveira is a collapsed entrance to the system located approximately 40 m above
170 the river's spring. The site contains a 6 m-thick Middle Palaeolithic sequence and has yielded a
171 total of nine Neanderthal skeletal elements (13), three of which are teeth (cf. Figs. S5-S6). One
172 of these teeth was recovered from layer 17, and the other two from layer 22, which is dated to
173 109.3 ± 28.4 ka by single grain optically stimulated luminescence and assigned an age of $93,250$
174 ± 3450 years via Bayesian modelling of the stratigraphic succession's chronological span; the
175 latter places layers 15-25, whose charcoal assemblage is dominated by the cold-adapted Scots
176 pine (*Pinus sylvestris*), in MIS-5b (32). The presence of characteristic Levallois stone tool
177 technology, an abundance of hearth material and tens of thousands of faunal remains (many of
178 them burnt) show that the site was used for the processing and consumption of locally hunted
179 fauna including rhino, horse, red deer, ibex, and tortoise (33-34).

180 The Galeria da Cisterna, which measures 100 m in length, opens approximately 5 m above the
181 extant spring and 35 m below the Gruta da Oliveira. Underlying a Holocene dark cave earth
182 deposit, it contains cemented sediment remnants of Last Glacial Maximum (LGM) and
183 Tardiglacial age. Level 3 of the AMD1 locus, a Magdalenian deposit dated on bone samples to
184 $10,820 \pm 60$ BP (GrA-9722; 12,708-12,882 cal BP) and $11,755 \pm 80$ BP (OxA-11129; 13,476-13,785
185 cal BP; Tables S2-S3) yielded fifteen human bone and dental specimens. Based on the
186 characteristics of the dental remains (cf. Fig. S7), it is suggested that a minimum of three
187 individuals of varying ages (young child to young adult) are represented. The small faunal
188 assemblage comprises red deer, Iberian ibex, and wild boar, along with smaller mammals such
189 as rabbit and hare (13, 35-36).

190 The Lapa dos Coelhos is a small cavity situated approximately 10 m above the Galeria da
191 Cisterna (Figs. S3-S4), containing two well preserved Magdalenian layers, 4 and 3, dated to,
192 respectively, $12,240 \pm 60$ BP (GrA-18377; on *Pinus sylvestris* charcoal) and $11,660 \pm 60$ BP (GrA-
193 18376; on a red deer bone), i.e., to between 13,353 and 14,803 cal BP (Tables S2-S3). A
194 substantial faunal assemblage was recovered from both layers, comprised primarily of rabbits,
195 red deer, Iberian ibex, and fish, mostly freshwater cyprinids (e.g., *Barbus* sp.) but including
196 *Salmo* sp. and *Alosa* sp. Analysis of the Magdalenian lithic assemblages and the presence of
197 bone artefacts interpreted as fishhooks in layer 4 has led to the interpretation of the site as a
198 temporary one, occupied intermittently for the exploitation of specific (and perhaps seasonal)
199 resources (35-38).

200 **Results**

201 The analysis of sediment leachates from 27 locations within the study area demonstrates a high
202 degree of geographical variation in $^{87}\text{Sr}/^{86}\text{Sr}$ values (Fig. 1 and Table S4). These range between
203 0.7081 (Sr-12) and 0.7362 (Sr-22), with less radiogenic values common along the Jurassic
204 limestone massif and more radiogenic values evident in the Neogene sedimentary basin of the
205 Tagus River and the Palaeozoic phyllites to the northeast of the Almonda karst system. Our
206 values are consistent with James et al.'s (39) large scale strontium isotope baseline map of
207 Portugal who give Sr isotope values in the range of 0.7082-0.7112 for the area incorporating the
208 Central Limestone Massif, the Neogene sedimentary basin and the Quaternary deposits
209 associated with the Tagus River.

210 The sequential strontium isotope data obtained for the two Neanderthal teeth from layer 22
211 (Oliveira 8 and Oliveira 9; Figs. S5-S6) are presented in Fig. 2. Both individuals exhibit
212 inhomogeneous strontium isotope profiles, with $^{87}\text{Sr}/^{86}\text{Sr}$ oscillating between minimum and
213 maximum values of approximately 0.7100 and 0.7115, respectively. Between four and five
214 different strontium isotope catchments can be observed in each profile, which can be accounted
215 for within the range of bioavailable strontium isotope values in the study area.

216 A selection of Mousterian fauna (Table S1) from different units of the Gruta da Oliveira MIS-5b
217 sequence, comprising horse (n=3), ibex (n=2), red deer (n=1) and *Stephanorhinus sp.* (n=2) was
218 also analysed, and the data are presented in Fig. S8. All three horse molars exhibit relatively
219 homogenous $^{87}\text{Sr}/^{86}\text{Sr}$ profiles with values ranging between 0.7095 and 0.7105, whilst the ibex
220 $^{87}\text{Sr}/^{86}\text{Sr}$ profiles oscillate between less radiogenic values of approximately 0.7086 and 0.7095.
221 The red deer $^{87}\text{Sr}/^{86}\text{Sr}$ values range between 0.7090 to 0.7095, whilst the two *Stephanorhinus sp.*
222 individuals exhibit more radiogenic values ranging between 0.7100 and 0.7115. Accompanying
223 oxygen isotope data obtained for two of the horse specimens, one ibex, one *Stephanorhinus sp.*
224 individual and the red deer specimen are plotted alongside the strontium isotope data.

225 The strontium isotope data obtained for the Magdalenian human premolar from Galeria da
226 Cisterna (Cisterna 2; Fig. S7) are presented in Fig. 2. Repeat oscillations between distinct values
227 of approximately 0.7095 and 0.7100 can be observed in the $^{87}\text{Sr}/^{86}\text{Sr}$ profile. To demonstrate its
228 primary position, the tooth was also directly dated (to $11,122 \pm 34$ BP; OxA-41,483, 12,926-
229 13,107 cal BP) (35-36) (Tables S2-S3).

230 An ibex maxilla (F3-88) and a red deer mandible (F3-72) from Magdalenian layer 4 of Lapa dos
231 Coelhos were selected to undergo analysis alongside the Cisterna 2 human tooth. To
232 demonstrate its primary position, the red deer mandible was directly dated (to $12,130 \pm 43$ BP;
233 OxA-41484; 13,811-14,115 cal BP) (35-36) (Tables S2-S3). The strontium and oxygen isotope
234 obtained are presented in Fig. S9. The ibex individual exhibits molar strontium isotope profiles
235 similar to those of the two Mousterian ibex, with values ranging between approximately 0.7086
236 and 0.7097. Two different isotope catchments can be observed in the red deer molars, with
237 values of 0.7103 and 0.7113.

238 Discussion

239

240 *Middle Palaeolithic*

241 The strontium isotope profiles of the two Neanderthals (Oliveira 8 and Oliveira 9) suggest that
242 these individuals engaged in systematic movement between four geological catchments during
243 M₃ and P₃ crown formation respectively (between 8.5 to 14.5 years, and 3.5 to 6.5 years (30).

244 The most radiogenic values observed in the enamel $^{87}\text{Sr}/^{86}\text{Sr}$ profiles of both individuals,
245 approximately 0.7112 to 0.7115, are consistent with the Neogene sedimentary basin that lies
246 between the Central Limestone Massif and the Tagus River (Sr-19, Sr-25, and Sr-28). The least
247 radiogenic value observed, approximately 0.7100, is consistent with strontium isotope values
248 observed in sediment leachates from Quaternary sedimentary deposits along the banks of the
249 Tagus River (Sr-2a). Based on the wider bioavailable strontium isotope mapping of the study
250 region, these values can be accounted for within a <20 km radius of the Almonda karst system.

251 To the north, north-east, and east, however, $^{87}\text{Sr}/^{86}\text{Sr}$ ratios are consistently above 0.7115
252 beyond a distance of 10-15 km from the site. We estimate the settlement-subsistence territory
253 as the largest circular or subcircular areas that satisfy the three conditions of (a) containing the
254 site, (b) containing terrain with soil Sr values consistent with those measured on the human
255 teeth, and (c) containing no terrain with soil Sr values inconsistent with those measured on the
256 human teeth (Fig. 3). This is c.600 km², mostly comprised of lowland alluvial terrain in the
257 Cenozoic basin of the Tagus and including the southern footslopes of the Serra d'Aire (Fig. 3);
258 this evidence suggests that, to north-east and east, the two individuals moved within an area
259 delimited by the drainage basin of the Atalaia stream (Fig. S2). These inferences are consistent
260 with the ranges suggested by studies of lithic raw material sourcing in the Mousterian deposits
261 of Gruta da Oliveira (40).

262 Sequential strontium and oxygen isotope data for Middle Palaeolithic fauna shows horse, red
263 deer and extinct rhinoceros were present in the two Neanderthals' subsistence territory all year
264 round, and the Iberian ibex intersects with this when they move to lower altitudes in the
265 summer. Horses, on the basis of their relatively homogenous enamel $^{87}\text{Sr}/^{86}\text{Sr}$ profiles (Fig S8;
266 representing 2-3 years of age [41]), likely occupied the alluvial plain along the right bank of the
267 Tagus River throughout the year (Sr-2a; Figs. 1,4). Seasonal variation is not readily apparent in
268 their $\delta^{18}\text{O}$ profiles, which likely reflects their behaviour as obligate drinkers (42) relying on the
269 waters of the Tagus and Almonda rivers, where seasonal $\delta^{18}\text{O}$ variation in local precipitation
270 may be dampened due to long residence times (42-43). Iberian ibex, on the other hand, are a
271 mountainous species highly adapted to life amongst steep, rocky slopes. The 2nd and 3rd molars
272 of our individuals likely represent formation times of around 12 months based on modern sheep
273 (45), and exhibit $^{87}\text{Sr}/^{86}\text{Sr}$ and $\delta^{18}\text{O}$ values that reflect seasonal movement between higher
274 altitudes in the Serra d'Aire and adjacent plateaus of the Central Limestone Massif (Sr-11 and Sr-
275 14; Fig. 4 and Fig. S8) and the lower altitudes at the source of the Almonda river (Sr-21b). This
276 seasonal movement is similar to that observed in modern populations (46), although their high
277 altitude-winter, low altitude-summer movements are the reverse of modern populations
278 elsewhere in Iberia. However, given that Serra d'Aire has a maximum altitude of c. 680 m, their
279 movement is probably driven by the availability of food rather than extreme winter cold.

280 On the basis of the consistency of their $^{87}\text{Sr}/^{86}\text{Sr}$ profiles with sediment leachate values Sr-19, Sr-
281 25, and Sr-28, the *Stephanorhinus sp.* individuals likely occupied the Neogene Tagus basin (Fig. 4
282 and Fig. S8), subsisting upon varying proportions of browse and grass depending on quality and
283 availability (47). Minimal intra-tooth variation in $\delta^{18}\text{O}$ of approximately 2‰ is evident, but does
284 not reflect seasonal signals, suggesting that these individuals likely obtained the majority of
285 their water from a source with a long oxygen residence time. The intra-tooth variation in
286 $^{87}\text{Sr}/^{86}\text{Sr}$ for both individuals may reflect a degree of movement between the banks of the Tagus
287 River and the Neogene basin. Similar small-scale seasonal mobility in *Stephanorhinus*

288 *kirchbergensis* has been observed in isotope data from an individual from western Poland,
289 where it is inferred that the individual spent the autumn months in more forested areas before
290 occupying more open areas in winter, spring, and summer (48). The $^{87}\text{Sr}/^{86}\text{Sr}$ profiles of the
291 single Middle Palaeolithic red deer specimen are similar to those of the sediment leachates from
292 the vicinity of the Almonda karst system (Sr-15, Sr-21b) and the Alvados polje (Sr-14) (Fig. 4 and
293 Figs. S2, S8). Little variation can be observed along the growth axes of either tooth, suggesting
294 that the individual likely subsisted entirely on the same geology during their formation. The $\delta^{18}\text{O}$
295 data for both teeth show an approximately 1‰ increase in values from the crown towards the
296 root, implying that the time period represented by these teeth was likely during the transition
297 from colder to warmer months.

298 **Upper Palaeolithic**

299 The sequential $^{87}\text{Sr}/^{86}\text{Sr}$ data for the Magdalenian individual from Galeria da Cisterna repeatedly
300 oscillate between two geologically distinct regions, consistent with sediment values from the
301 source of the Almonda River (Sr-21b) and the banks of the Tagus River (Sr-2a), of which the
302 Almonda is a tributary. The ranging distance of the Magdalenian individual during the period of
303 dental formation therefore falls within approximately 20 km of the Galeria da Cisterna and could
304 well represent back-and-forth movement along the right bank of the river valley (Figs. 2-3),
305 between spring (at the Almonda escarpment) and mouth (at the confluence with the Tagus).
306 The size of the corresponding subsistence territory, estimated as above, is $\sim 300 \text{ km}^2$. This is in
307 line with observations of raw material procurement in the contemporaneous Magdalenian
308 layers of the adjacent Lapa dos Coelhos site; $\sim 80\%$ of which comes from sources in the
309 intermediate Neogene terrain (37).

310 Like the Mousterian ibex specimens from Gruta da Oliveira, the strontium and oxygen isotope
311 data suggest that the Magdalenian ibex individual from Lapa dos Coelhos (F3-88) engaged in
312 some form of seasonal altitudinal mobility (Fig. 4 and Fig. S9) between higher altitudes on the
313 Serra d’Aire (Sr-14, Sr-11) in winter and lower altitudes in the vicinity of the Almonda karst
314 system in summer (Sr-15; Sr-21b), where it intersects with the proposed subsistence territory
315 for the Magdalenian individual. The intra-tooth $\delta^{18}\text{O}$ variation is approximately 4‰, though in
316 this relatively low altitude terrain, the greater extent of oxygen isotope variation when
317 compared to the Mousterian ibex may suggest more seasonal extremes in temperature during
318 the Tardiglacial than during MIS 5b. The strontium isotope profiles obtained for the M1, M2 and
319 M3 of the Magdalenian red deer from Lapa dos Coelhos (F3-72) are consistent with mobility
320 between two distinct geologies (Fig. 4 and Fig. S9). The least radiogenic values fall within those
321 of sediment leachates from the banks of the Tagus River (Sr-2a), within the proposed
322 subsistence territory of the human individual and correspond to the warmer months. The
323 highest are consistent with areas of the Neogene sediments of the Tagus basin (Sr-19, Sr-28)
324 that may lie outside the subsistence territory. $\delta^{18}\text{O}$ values are similar to the ibex, with intra-
325 tooth variation approximately 4‰, and with the highest oxygen isotope values corresponding to
326 the least radiogenic $^{87}\text{Sr}/^{86}\text{Sr}$ troughs and the lowest oxygen isotope values corresponding to the
327 most radiogenic $^{87}\text{Sr}/^{86}\text{Sr}$ peaks. This may reflect a degree of local seasonal mobility, perhaps in
328 response to the seasonal availability of good forage.

329 Both the red deer and ibex are present for at least part of the year in the subsistence territory
330 proposed for the Magdalenian individual, with their strontium isotope values overlapping with
331 the two strontium isotope catchments identified in the human tooth (Figs. 3-4). The cyclical

332 movement of Cisterna 2 between two different geological catchments is suggestive of seasonal
333 movement, and did not include the limestone mountains and plateaus extending to north and
334 north-west of the Almonda escarpment. The presence of fishhooks and fish vertebra, and direct
335 evidence for the consumption of aquatic resources provided by $\delta^{13}\text{C}$ and $\delta^{15}\text{N}$ (-18.65‰ and
336 10.89‰ respectively, Fig. S11) indicate the importance of freshwater aquatic resources and a
337 small marine input likely from the anadromous fish (*Salmo* sp. and *Alosa* sp.) represented in the
338 bone assemblage (37). The movement between riparian locations on the Almonda and Tagus
339 rivers might be linked to the importance of these resources.

340

341 The continuity between the Middle and the late Upper Palaeolithic in the presence and location
342 of some of the prey species suggests that the marked differences in human movement and
343 subsistence territory between the two periods is unlikely to have been determined by changes
344 in ecology. This is supported by paleobotanical evidence. *Pinus sylvestris* is the dominant taxon
345 in the charcoal assemblage from the MIS 5b levels of Gruta da Oliveira and is also well
346 represented in the Upper Magdalenian of the region, namely in layer 4 of Lapa dos Coelhos and
347 in coeval layer F of Lapa do Picareiro, 5 km to the north across the Serra d'Aire (38, 49-50).
348 Nowadays restricted to the high mountains of Portugal, above 1500 m, this taxon denotes the
349 altitudinal compression of vegetation belts under colder climatic conditions and is a proxy for a
350 Scots pine-and-heathland open landscape across the lowlands of Portuguese Estremadura (49).

351

352 Against a comparable landscape setting, horses, well represented in Solutrean layer 8 of Lapa
353 dos Coelhos), are absent from the Almonda karst's Upper Magdalenian faunal assemblages
354 (Galeria da Cisterna and layers 3-4 of Lapa dos Coelhos) (14, 37). A similar trend is apparent at
355 Lapa do Picareiro, where horses are present through Gravettian levels T-Z but absent from
356 Upper Magdalenian level F/G, whose abundant faunal remains are of rabbit (97%), red deer
357 (2%) and wild boar (1%), and include a few hundred fish bones of the same taxa represented at
358 Lapa dos Coelhos (52-54). A reduction in subsistence territory in the Magdalenian might
359 therefore explain the absence of horses in the faunal assemblage. Horses were extensively
360 hunted in preceding periods, and persisted in the region until the early-mid Holocene (55), but
361 are not present in the Galeria da Cisterna and Lapa dos Coelhos assemblages. Either
362 the Magdalenians' restricted territory did not overlap with horses, or horses were butchered
363 and consumed away from the Almonda caves.

364

365 Consideration of exchange networks as revealed by the occurrence of shell ornaments in the
366 Upper Palaeolithic of central Portugal is also consistent with a marked contraction of territories
367 in the Tardiglacial. In the Upper Magdalenian, such ornaments are almost entirely of freshwater
368 taxa. In the Solutrean and the Gravettian, despite a much lower sea level making for a
369 significantly greater geographical separation between littoral and inland groups, shell beads are
370 overwhelmingly of marine taxa (*SI Appendix*, Text S5).

371

372 The abundance of fish and rabbit remains in the regional Upper Magdalenian suggests that
373 people were moving down the food chain to accommodate a decrease in territory size,
374 presumably as a consequence of growth in population numbers and population density. A
375 similar argument has been put forth based on the subsistence importance acquired in the
376 Tardiglacial (for the first time in the Palaeolithic of Europe) by the regular exploitation of
377 freshwater fish apparent in broadly coeval French and Italian sites (56-58.) The increase in

378 archaeological site frequency per millennium observed through the Middle and the Upper
379 Palaeolithic of northern Spain and SW France is consistent with these inferences (59-60).

380

381 The subsistence territory estimated for the Upper Palaeolithic human from Galeria da Cisterna is
382 about half the area of that proposed for the two Neanderthals from Gruta da Oliveira. It
383 represents the opposite trend to the more than two-fold increase in home-range between the
384 Middle Paleolithic and Late Upper Palaeolithic estimated for SW France and the northern
385 European plain based on raw material sourcing (61). This contrast is to be expected, given the
386 lower latitude of central Portugal and the littoral location of the study area, which is far beyond
387 the Eurasian steppe-tundra domain. This geography would also have made for the impact of
388 climate oscillations to be lesser and for the carrying capacity of the land to be up to one order of
389 magnitude greater than in European regions to the north of the Pyrenees — for the 13-15 ka cal
390 BP interval, climate envelope modeling estimates are that central Portugal could have
391 supported population densities of up to 16-23 people/100 km² (62). Based on these estimates,
392 the model Upper Magdalenian territory derived from the strontium evidence could have
393 harboured up to 50-70 people and so would have been big enough to sustain a hunter-gatherer
394 band of typical size.

395

396

397 **Conclusions**

399 Here we present highly spatially resolved sequential strontium isotope data for two Middle
400 Palaeolithic humans and one Upper Palaeolithic human from the Almonda karst system in
401 Portuguese Estremadura. Sequential strontium and oxygen isotope analysis of Middle and
402 Upper Palaeolithic fauna suggest that all four species sampled (ibex, red deer, horse, and rhino)
403 were either resident or seasonally available within a short distance from the Almonda karst
404 sites. Data for Middle Palaeolithic horses and red deer suggest little to no mobility during
405 enamel formation, whilst Middle Palaeolithic rhino engaged in small-scale, local mobility that
406 may have been seasonal in nature. Upper Palaeolithic red deer were also seasonally mobile
407 across the study area during dental formation, and both Middle and Upper Palaeolithic ibex
408 engaged in altitudinal mobility.

409 Based on ⁸⁷Sr/⁸⁶Sr mapping of the study area, we conclude that the Neanderthal individuals
410 occupied a subsistence territory of ~600 km², and likely subsisted on four geological catchments
411 that were visited and revisited within a 10-15 km radius of the Almonda spring, consistent with a
412 settlement-subsistence system leaning towards Binford's "forager" model of mobility (63), and
413 with suggestions that Neanderthals may have had high basal metabolic rates, requiring them to
414 make frequent but short distance forages (64). In contrast, the Magdalenian individual subsisted
415 primarily upon resources obtained, probably seasonally, from two geological catchments along a
416 20 km stretch of the right bank of the Almonda River, between the spring and the mouth,
417 representing a subsistence territory of ~300 km². Whilst we recognize that a switch in diet in the
418 Magdalenian to high strontium local resources (e.g. fish or freshwater molluscs) may mask the
419 true extent of the subsistence territory, we see no evidence in the enamel for covariance of Sr
420 isotopic values with Sr concentrations, which we would predict if this was the case (see
421 Supplementary Information).

422

423 The reduction in territory size inferred from our sequential strontium isotope data may be
424 related to increased population density during the late Upper Palaeolithic. Future in-situ oxygen
425 isotope analysis of the human tooth enamel, e.g. (65), may enable us to better understand the
426 seasonal timescales involved in this process.

427

428

429 **Acknowledgments**

430

431 BL was supported by an AHRC SWWDTP scholarship. AWGP's research was supported by a Royal
432 Society Wolfson Research Merit Award. Radiocarbon dates were funded by NEIF Project
433 2386.0321. The authors would like to thank Paul Pettitt and Chris Standish for their help
434 collecting the sediment samples, as well as Erik Trinkaus, John Willman, Simon Davis, and
435 Cristina Gameiro for their help with the selection of the human and faunal samples.

436

437 **References**

438

- 439 1. T. Higham *et al.*, The timing and spatiotemporal patterning of Neanderthal disappearance.
440 *Nature* **512**, 306-309 (2014).
- 441 2. T. Aubry *et al.*, Timing of the Middle-to-Upper Palaeolithic transition in the Iberian inland
442 (Cardina-Salto do Boi, Côa Valley, Portugal). *Quaternary Research* **98**, 81-101 (2020).
- 443 3. L. G. Straus, Neanderthal last stand? Thoughts on Iberian refugia in late MIS 3. *Journal of*
444 *Quaternary Science* **37**, 283-290 (2022).
- 445 4. J. Maroto *et al.*, Current issues in late Middle Palaeolithic chronology: New assessments
446 from Northern Iberia. *Quaternary International* **247**, 15-25 (2012).
- 447 5. J. Zilhão, Neandertals and moderns mixed, and it matters. *Evolutionary Anthropology* **15**,
448 183-195 (2006).
- 449 6. J. Zilhão, The late persistence of the Middle Palaeolithic and Neandertals in Iberia: A review
450 of the evidence for and against the “Ebro Frontier” model. *Quaternary Science Reviews* **270**,
451 107098 (2021).
- 452 7. R. A. Bentley, Strontium isotopes from the earth to the archaeological skeleton: a review.
453 *Journal of Archaeological Method and Theory* **13**, 135-187 (2006).
- 454 8. H. De Jong, G. Foster, V. Heyd, A. W. Pike, “Further Sr isotopic studies on the Eulau multiple
455 graves using laser ablation ICP-MS” in *Anthropologie, Isotopie und DNA—biografische*
456 *Annäherung an namenlose vorgeschichtliche Skelette*. H. Meller, K. W. Alt, Eds. (Landesamt
457 für Denkmalpflege und Archäologie Sachsen-Anhalt - Landesmuseum für Vorgeschichte,
458 Halle, 2010), pp. 53-62.
- 459 9. M. Willmes *et al.*, Improvement of laser ablation in situ micro-analysis to identify diagenetic
460 alteration and measure strontium isotope ratios in fossil human teeth. *Journal of*
461 *Archaeological Science* **70**, 102-116 (2016).
- 462 10. S. Mays *et al.*, Lives before and after Stonehenge: An osteobiographical study of four
463 prehistoric burials recently excavated from the Stonehenge World Heritage Site. *Journal of*
464 *Archaeological Science: Reports* **20**, 692-710 (2018).
- 465 11. H. De Jong, *Subsistence plasticity: A strontium isotope perspective on subsistence through*
466 *intra-tooth enamel and inter-site variation by LA-MC-ICPMS and TIMS*. PhD, University of
467 Bristol (2013).
- 468 12. J. Daura *et al.*, New Middle Pleistocene hominin cranium from Gruta da Aroeira (Portugal).
469 *Proceedings of the National Academy of Sciences* **114**, 3397-3402 (2017).

- 470 13. J. C. Willman, J. Maki, P. Bayle, E. Trinkaus, J. Zilhão, Middle Paleolithic Human Remains
471 from the Gruta da Oliveira (Torres Novas), Portugal. *American Journal of Physical*
472 *Anthropology* **149**, 39-51 (2012).
- 473 14. E. Trinkaus, S. Bailey, S. J. Davis, J. Zilhão, Magdalenian human remains from the Galeria da
474 Cisterna (Almonda karstic system, Torres Novas, Portugal). *O Arqueólogo Português* **V-1**,
475 395-413 (2011).
- 476 15. J. Zilhão *et al.*, Revisiting the Middle and Upper Palaeolithic archaeology of Gruta do
477 Caldeirão (Tomar, Portugal). *PLoS One* **16**, e0259089 (2021).
- 478 16. J. Montgomery, Passports from the past: investigating human dispersals using strontium
479 isotope analysis of tooth enamel. *Annals of Human Biology* **37**, 325-346 (2010).
- 480 17. D. T. Flockhart, T. K. Kyser, D. Chipley, N. G. Miller, D. R. Norris, Experimental evidence
481 shows no fractionation of strontium isotopes ($^{87}\text{Sr}/^{86}\text{Sr}$) among soil, plants, and
482 herbivores: implications for tracking wildlife and forensic science. *Isotopes in Environmental*
483 *and Health Studies* **51**, 372-381 (2015).
- 484 18. J. Lewis, A. W. G. Pike, C. D. Coath, R. P. Evershed, Strontium concentration, radiogenic
485 ($^{87}\text{Sr}/^{86}\text{Sr}$) and stable ($\delta^{88}\text{Sr}$) strontium isotope systematics in a controlled feeding study.
486 *STAR: Science & Technology of Archaeological Research* **3**, 45-57 (2017).
- 487 19. S. D. Blaschko *et al.* Strontium substitution for calcium in lithogenesis. *The Journal of*
488 *Urology* **189**, 735-739 (2013).
- 489 20. S. Hillson, *Teeth* (Cambridge University Press, Cambridge, 1986).
- 490 21. J. E. Ericson, Strontium isotope characterization in the study of prehistoric human
491 ecology. *Journal of Human Evolution* **14**, 503-514 (1985).
- 492 22. K. Jaouen, M. P. Richards, A. Le Cabec, F. Welker, W. Rendu, J. J. Hublin, M. Soressi, S.
493 Talamo. Exceptionally high $\delta^{15}\text{N}$ values in collagen single amino acids confirm Neandertals
494 as high-trophic level carnivores. *Proceedings of the National Academy of Sciences* **116**(11),
495 4928-4933 (2019).
- 496 23. D. González-Weller, D. et al., Dietary intake of barium, bismuth, chromium, lithium, and
497 strontium in a Spanish population (Canary Islands, Spain). *Food and Chemical Toxicology* **62**,
498 856-868 (2013).
- 499 24. L. L. Gourcy, M. Groening, P. K. Aggarwal, "Stable oxygen and hydrogen isotopes in
500 precipitation" in *Isotopes in the Water Cycle* (Springer, Dordrecht, 2005), pp. 39-51.
- 501 25. M. Balasse, A. B. Smith, S. H. Ambrose, S. R. Leigh, Determining sheep birth seasonality by
502 analysis of tooth enamel oxygen isotope ratios: the Late Stone Age site of Kasteelberg
503 (South Africa). *Journal of Archaeological Science* **30**, 205-215 (2003).
- 504 26. K. Britton, V. Grimes, J. Dau, M. P. Richards, Reconstructing faunal migrations using intra-
505 tooth sampling and strontium and oxygen isotope analyses: a case study of modern caribou
506 (*Rangifer tarandus granti*). *Journal of Archaeological Science* **36**, 1163-1172 (2009).
- 507 27. J. Montgomery, J. A. Evans, M. S. Horstwood, Evidence for long-term averaging of strontium
508 in bovine enamel using TIMS and LA-MC-ICP-MS strontium isotope intra-molar
509 profiles. *Environmental Archaeology* **15**, 32-42 (2010).
- 510 28. N. Lazznerini *et al.*, A. Monthly mobility inferred from isoscapes and laser ablation strontium
511 isotope ratios in caprine tooth enamel. *Scientific Reports* **11**, 2277 (2021).
- 512 29. T. M. Smith *et al.*, Wintertime stress, nursing, and lead exposure in Neanderthal children.
513 *Science Advances* **4**, eaau9483.

- 514 30. S. J. AlQahtani, M. P. Hector, H. M. Liversidge, Brief communication: the London atlas of
515 human tooth development and eruption. *American Journal of Physical Anthropology* **142**,
516 481-490 (2010).
- 517 31. A. Boethius, T. Ahlström, M. Kielman-Schmitt, M. Kjällquist, L. Larsson, Assessing laser
518 ablation multi-collector inductively coupled plasma mass spectrometry as a tool to study
519 archaeological and modern human mobility through strontium isotope analyses of tooth
520 enamel. *Archaeological and Anthropological Sciences* **14**, 97 (2022).
- 521 32. J. Zilhão *et al.*, A revised, Last Interglacial chronology for the Middle Palaeolithic sequence
522 of Gruta da Oliveira (Almonda karst system, Torres Novas, Portugal). *Quaternary Science*
523 *Reviews* **258**, 106885 (2021)
- 524 33. J. Zilhão *et al.* "Humans and hyenas in the Middle Paleolithic of Gruta da Oliveira (Almonda
525 karstic system, Torres Novas, Portugal)" in Actas de la 1ª Reunión de científicos sobre
526 cubiles de hiena (y otros grandes carnívoros) en los yacimientos arqueológicos de la
527 Península Ibérica (Museo Arqueológico Regional, Alcalá de Henares, 2010), 298-308.
- 528 34. M. Nabais, J. Zilhão, The consumption of tortoise among Last Interglacial Iberian
529 Neanderthals. *Quaternary Science Reviews* **217**, 225-246 (2019).
- 530 35. P. J. Reimer *et al.*, The IntCal20 Northern Hemisphere Radiocarbon Age Calibration Curve
531 (0–55 cal kBP). *Radiocarbon* **62**, 725-757 (2020).
- 532 36. M. Stuiver, P. J. Reimer, Extended 14C data base and revised CALIB 3.0 14C age calibration
533 program. *Radiocarbon* **35**, 215-230 (1993).
- 534 37. C. Gameiro, S. Davis, F. Almeida, "A sequência estratigráfica da Lapa dos Coelhos:
535 funcionalidade e subsistência ao longo do Pleistocénico Superior no sopé na Serra de Aire
536 (Portugal)" in Arqueologia em Portugal. 2017 - Estado da Questão, J. M. Arnaud, A. Martins,
537 Eds. (Associação dos Arqueólogos Portugueses, Lisboa, 2017), pp. 357-374.
- 538 38. F. Almeida, D. E. Angelucci, C. Gameiro, J. Correia, T. Pereira, Novos dados para o Paleolítico
539 Superior final da Estremadura portuguesa: resultados preliminares dos trabalhos
540 arqueológicos de 1997-2003 na Lapa dos Coelhos (Casais Martanes, Torres Novas).
541 *Promontoria* **2**, 157-192 (2004).
- 542 39. H. F. James *et al.*, A large-scale environmental strontium isotope baseline map of Portugal
543 for archaeological and paleoecological provenance studies. *Journal of Archaeological Science*
544 **142**, 105595 (2022).
- 545 40. H. Matias, Raw material sourcing in the Middle Paleolithic site of Gruta da Oliveira (Central
546 Limestone Massif, Estremadura, Portugal). *Journal of Lithic Studies* **3**, 541-560 (2016).
- 547 41. K. Hoppe, M. Stover, J. Pascoe, R. Amundson, Tooth enamel biomineralization in extant
548 horses: implications for isotopic microsampling. *Palaeogeography, Palaeoclimatology,*
549 *Palaeoecology* **206**, 355-365 (2004).
- 550 42. D. Goodwin, "Horse behaviour: evolution, domestication and feralization" in The welfare of
551 horses (Springer, Dordrecht, 2007), pp. 1-18.
- 552 43. C. D. Kennedy, G. J. Bowen, J. R. Ehleringer, Temporal variation of oxygen isotope ratios
553 ($\delta^{18}O$) in drinking water: implications for specifying location of origin with human scalp
554 hair. *Forensic Science International* **208**, 156-166 (2011).
- 555 44. S. Pederzani, K. Britton, Oxygen isotopes in bioarchaeology: Principles and applications,
556 challenges and opportunities. *Earth-Science Reviews* **188**, 77-107 (2019).
- 557 45. A. Zazzo *et al.*, The isotope record of short-and long-term dietary changes in sheep tooth
558 enamel: implications for quantitative reconstruction of paleodiets. *Geochimica et*
559 *Cosmochimica Acta* **74**, 3571-3586 (2010).

- 560 46. P. Acevedo, J. Cassinello, Biology, ecology and status of Iberian ibex *Capra pyrenaica*: a
561 critical review and research prospectus. *Mammal Review* **39**, 17-32 (2009).
- 562 47. E. N. van Asperen, R. D. Kahlke, Dietary variation and overlap in Central and Northwest
563 European *Stephanorhinus kirchbergensis* and *S. hemitoechus* (Rhinocerotidae, Mammalia)
564 influenced by habitat diversity: “You’ll have to take pot luck!”(proverb). *Quaternary Science*
565 *Reviews* **107**, 47-61 (2015).
- 566 48. K. Stefaniak *et al.*, Browsers, grazers or mix-feeders? Study of the diet of extinct Pleistocene
567 Eurasian forest rhinoceros *Stephanorhinus kirchbergensis* (Jäger, 1839) and woolly
568 rhinoceros *Coelodonta antiquitatis* (Blumenbach, 1799). *Quaternary International* **605-606**,
569 192-212 (2020).
- 570 49. E. Badal, V. Villaverde, J. Zilhão, “Middle Palaeolithic wood charcoal from three sites in
571 South and West Iberia: biogeographic implications” in Wood and charcoal. Evidence for
572 human and natural History, E. Badal, Y. Carrión, M. Macías, M. Ntinou, Eds. (Universitat de
573 València, València, 2012), pp. 13-24.
- 574 50. N. F. Bicho, J. Haws, B. Hockett, A. Markova, W. Belcher, Paleoecologia e ocupação humana
575 da Lapa do Picareiro: resultados preliminares. *Revista Portuguesa de Arqueologia* **6**, 49-81
576 (2003).
- 577 51. P. F. Queiroz, J. E. Mateus, W. Van Leeuwen, “The Paleovegetational Context” in
578 Portrait of the Artist as a Child. The Gravettian Human Skeleton from the Abrigo do Lagar
579 Velho and its Archeological Context. (Instituto Português de Arqueologia, Lisboa, 2002), pp.
580 92-111.
- 581 52. N. F. Bicho, B. Hockett, J. Haws, W. Belcher, Hunter–gatherer subsistence at the end of the
582 Pleistocene: preliminary results from Picareiro Cave, Central Portugal. *Antiquity* **74**, 500-506
583 (2000).
- 584 53. N. Bicho, J. Haws, B. Hockett, Two sides of the same coin—rocks, bones and site function of
585 Picareiro Cave, central Portugal. *Journal of Anthropological Archaeology* **25**, 485-499
586 (2006).
- 587 54. J. Haws *et al.*, Human adaptive responses to climate and environmental change during the
588 Gravettian of Lapa do Picareiro (Portugal). *Quaternary International* **587-588**, 4-18 (2021).
- 589 55. A. Lentacker, Preliminary results of the fauna of Cabeço de Amoreira and Cabeço de Arruda
590 (Muge, Portugal). *Trabalhos de Antropologia e Etnologia* **26** (1986).
- 591 56. E. L. Jones, Climate change, patch choice, and intensification at Pont d'Ambon (Dordogne,
592 France) during the Younger Dryas. *Quaternary Research* **72**, 371-376 (2009).
- 593 57. H. Russ, A. K. G. Jones, Late Upper Palaeolithic fishing in the Fucino Basin, central Italy, a
594 detailed analysis of the remains from Grotta di Pozzo. *Environmental Archaeology* **14**, 155-
595 162 (2009).
- 596 58. J. Zilhão, “The Upper Palaeolithic of Europe” in The Cambridge World Prehistory, C.
597 Renfrew, P. Bahn, Eds. (Cambridge University Press, Cambridge, 2014), vol. 3, pp. 1753-
598 1785.
- 599 59. L. G. Straus, *Iberia before the Iberians* (University of New Mexico Press, Albuquerque,
600 1992).
- 601 60. J. C. French, The demography of the Upper Palaeolithic hunter–gatherers of Southwestern
602 France: A multi-proxy approach using archaeological data. *Journal of Anthropological*
603 *Archaeology* **39**, 193-209 (2015).

- 604 61. Gamble, C., J. Steele, “Hominid ranging patterns and dietary strategies” in Hominid
605 evolution: Lifestyles and survival strategies, H. Ullrich, Ed., (Gelsenkirchen, Edition Archaea,
606 1999), pp. 346–409.
- 607 62. M. Tallavaara, M. Luoto, N. Korhonen, H. Järvinen, H. Seppä, Human population dynamics
608 in Europe over the Last Glacial Maximum. *Proceedings of the National Academy of Sciences*
609 **112**, 8232-8237 (2015).
- 610 63. L. Binford, *In pursuit of the past: Decoding the archaeological record* (Thames and Hudson,
611 London, 1983).
- 612 64. A. Verpoorte, Neanderthal energetics and spatial behaviour. *Before Farming*, **3**, 1-6 (2006).
- 613 65. M. Aubert *et al.* In situ oxygen isotope micro-analysis of faunal material and human teeth
614 using a SHRIMP II: a new tool for palaeo-ecology and archaeology. *Journal of Archaeological*
615 *Science* **39**, 3184-3194 (2012).
- 616 66. J. J. C. Pais (2010) Carta Geológica de Portugal à escala 1:1 000 000. (Laboratório Nacional
617 de Energia e Geologia, Amadora).
618

619 Figures

620

621 **Figure 1.** Geological map of the sampled area, whose position in Iberia is indicated by the
622 rectangle in the insert. The star denotes the Almonda spring. Sampling spots are indicated by
623 their number and mean $^{87}\text{Sr}/^{86}\text{Sr}$ value (Table S4). 1. Holocene sands, gravel, silts, and clays; 2.
624 Pleistocene conglomerates, sandstones, siltstones and claystones; 3. Pliocene sandstones,
625 siltstones and claystones; 4. Miocene sandstones, claystones, conglomerates, and limestones; 5.
626 Palaeogene sandstones, conglomerates, claystones, and siltstones; 6. Upper Cretaceous
627 limestones, sandstones, marl, and dolomites; 7. Lower Cretaceous sandstones, limestones, marl,
628 and dolomites; 8. Upper Jurassic limestones, marl, and sandstones; 9. Middle Jurassic
629 limestones, marl, and dolomites; 10. Lower Jurassic limestones, marl, and dolomites; 11. Triassic
630 sandstones, claystones, and evaporites; 12. Silurian phyllites, shales, and metacherts; 13.
631 Ordovician quartzites, quartzophyllites, and metaconglomerates; 14. Cambrian schists, gneisses,
632 migmatites and amphibolites; 15. Neoproterozoic phyllites, metacherts, metaconglomerates
633 and shales; 16. Neoproterozoic schists, gneisses, metacherts, migmatites, and amphibolites; 17.
634 Deformed orthogneisses, granites and diorites. After (66).

635 **Figure 2.** Sequential $^{87}\text{Sr}/^{86}\text{Sr}$ enamel profiles, obtained through LA-MC-ICP-MS analysis, of the
636 three human teeth analysed, plotted from left (top of crown) to right (enamel cervix), following
637 the growth axis.

638

639 **Figure 3.** Modelled territories used by the Oliveira and Cisterna individuals. The star denotes
640 the Almonda spring. The red dots denote the sampling localities within the delimited areas
641 where soil leachates yielded Sr values consistent with the human values. The circular area
642 modelled for the Mousterian (~600 km²) is bounded by points Sr-25 (0.7112) and Sr-2a (0.7100),
643 consistent, and Sr-5 (0.7172), inconsistent, with the human tooth values. The elliptical area
644 modelled for the Magdalenian (~300 km²) is bounded by points Sr-21b (0.7095) and Sr-2a
645 (0.7100), consistent, and Sr-1a (0.7130) and Sr-19 (0.7113), inconsistent, with the human tooth
646 values. Through the timespan of their enamel formation, the two Mousterian individuals
647 roamed across the Tagus basin and ventured into the Massif, while the Magdalenian individual

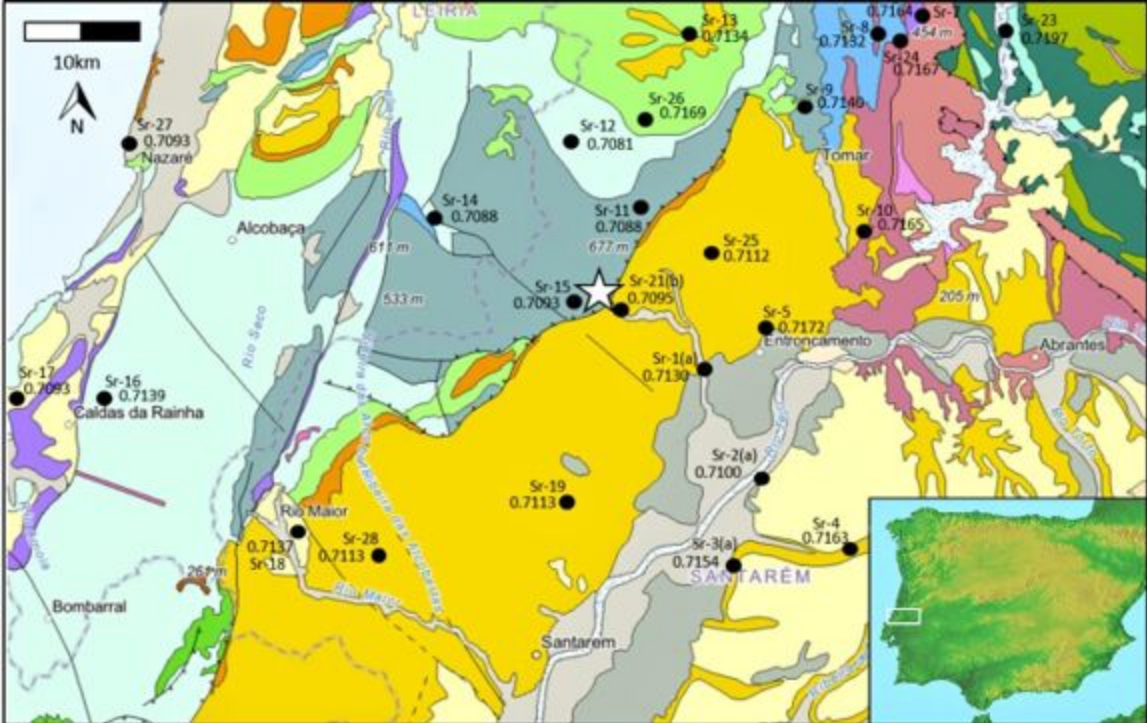
648 moved regularly across a territory half the size that would not seem to have included the Massif
649 and corresponds to terrain along the right bank of River Almonda. Given the predominantly
650 plant source of dietary strontium, our results do not rule out hunting forays outside these
651 ranges, but we have also shown that important prey species are present within these ranges for
652 at least part or all of the year.

653

654 **Figure 4.** Potential ranges of the main Middle and Upper Palaeolithic animal prey species
655 represented in the Almonda karst sites, as indicated, for each taxon, by the sampling localities
656 (red dots) where soil leachates yielded Sr values (indicated) within the range of the tooth values.
657 The star denotes the Almonda spring. Elevations are colour-coded as in Fig. 3.

658

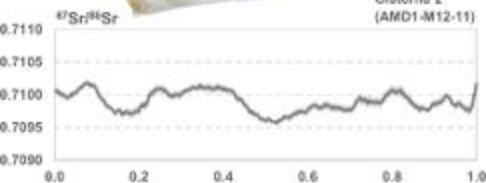
659



Laser track

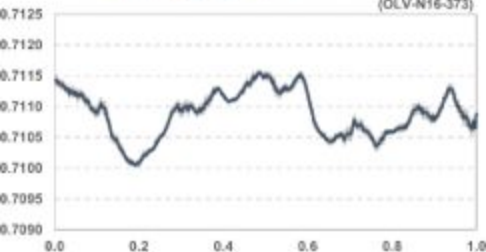


Cisterna 2
(AMD1-M12-11)



Laser tracks

Oliveira 8
(OLV-N16-373)

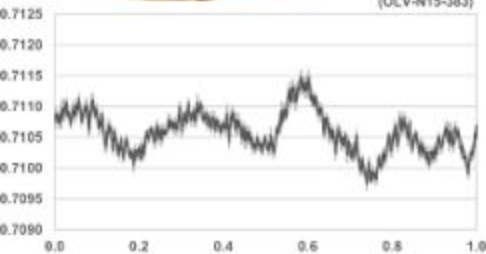


Enamel

Dentine

Laser tracks

Oliveira 9
(OLV-N15-383)



Relative distance along enamel

